Synthesis of Mn2+-doped CdS nanoparticles covered with different adsorptive layers and their application as biosensors

V.I. Fediv[1], G.Yu. Rudko[2], A.I. Savchuk[3], E.G. Gule[2], I.S. Davydenko[1], O.I. Olar[1], K.S. Volkov[4]
[1]*Bukovinian State Medical University, Department of Biophysics and Medical Informatics,*
42, Kobylianska str., 58000 Chernivtsi, Ukraine,
[2]*V. Lashkaryov Institute of Semiconductor Physics, National Academy of Sciences of Ukraine,*
45, prospect Nauky, 03028 Kyiv, Ukraine,
[3]*Chernivtsi National University, 2, Kotsyubynsky str., 58012 Chernivtsi, Ukraine*
[4]*I.Ya. Horbachevsky Ternopil State Medical University*

Abstract. Colloidal CdS:Mn nanoparticles were synthesized in water solutions of the polymer polyvinyl-pyrrolidone (PVP), the surfactant cetyl-trimethyl-ammonium bromide (CTAB) and the mixture of PVP and CTAB. The sizes of nanoparticles were determined by electron microscopy and optical absorption methods. The growth media influence on photoluminescence of nanoparticles has been studied. It has been shown that the chemical composition and structure of the adsorptive layer on the surface of nanoparticles can be used as a technological tool to control their light emission. The possibility to use CdS:Mn NPs grown in PVP as light-emitting labels in biological media has been demonstrated.

1. Introduction

The novel properties of complex materials outperform those of the individual components, and, thus, attract a lot of attention in view of ample applications in various fields. Recently, the interest has been focused on the new family of such materials – the inorganic nanoparticles (NPs) embedded in organic (e.g., polymeric) matrices. The hybrid nature of these materials greatly expands the possibilities for property control: the size-dependent manipulation of NPs properties is complemented by the variation of organic components and optimization of the interfacial interactions in the hybrid.

Colloidal chemistry methods are widely used to synthesize the hybrid nanomaterials because they are cheap and easy to upscale, and NPs obtained are highly versatile in terms of composition, size, shape and surface control. Due to all these advantages the multitude of colloidal NPs emerge in optoelectronics, photonics, catalysis, solar energy conversion, and biomedical sensing [1]. In particular, semiconductor NPs have been proposed as fluorescent labels that open up new possibilities for biomolecular and cellular imaging [2]. The strengths of these nanoprobes are based on the higher photostability of NPs as compared to traditionally used dyes, which guarantees the observation of biomolecules over longer time periods, on their broad excitation and size-tunable

emission properties, on large absorption coefficients, etc. [3-5]. Introduction of localized magnetic ions in semiconductor NPs leads to new manipulation possibilities; e.g., doping with Mn^{2+} leads, due to exchange interactions between s,p band electrons and the Mn^{2+} d electrons, both to new magnetic characteristics and new light-emitting transitions related to Mn^{2+} ions [6].

Notably, using NPs in biology and medicine greatly depends on the compatibility of these probes with organic environments. Interactions with various organic components can modify the interface of NPs and, thus, change the photoluminescence (PL) properties of NPs [7], which can deteriorate the function of sensing.

The object of the present work was to synthesize NPs with different organic surface layers, to study their specific characteristics, to find out the consistent patterns of the effect of the chemical nature and the structure of the adsorbed layer on the characteristics of CdS:Mn nanoparticles, and to find out whether synthesized CdS:Mn NPs can be used for creation of light-emitting biosensors.

2. Experimental

Nanoparticles CdS:Mn were synthesized in polyvinyl-pyrrolidone (PVP) by chemical precipitation route in the water solutions containing ions Cd^{2+}, Mn^{2+}, S^{2-}, polymer polyvinyl-pirrolidon and/or surfactant cetyl-trimethyl-ammonium bromide (CTAB). The salts cadmium chloride ($CdCl_2$), sodium sulfide (Na_2S), and manganese chloride ($MnCl_2$) were of the analytical grade and were used with no further purification. The solutions of these salts in the concentration 0.1 mol/g were prepared using the bidistilled water. Concentrations of PVP and CTAB in the solutions were 5 mas.% and 0.1 mol/dm^3, respectively. To synthesize nanocomposites of different compositions, i.e. PVP/CdS:Mn, CTAB/CdS:Mn and (PVP+CTAB)/CdS:Mn, we used the following synthesis procedures: precipitation of NPs in the water solution of PVP (1); CTAB (2); mixture PVP+CTAB (3).

Optimal synthesis conditions (pH value and precursors concentrations) were chosen in accordance with [8] to avoid formation of the precipitates of MnS, $Mn(OH)_2$ and $Cd(OH)_2$ and to provide the colloidal solution containing CdS:Mn NPs. The concentration of Mn^{2+} ions in the synthesis solutions was $5 \cdot 10^{-3}$ M, concentrations of Cd^{2+} ions and CTA^+ were varied, respectively, within the range 1…30 мM and 0.5…10 мM, and the concentration of PVP was 5 mas.% in all synthesis procedures.

All the colloidal solutions were further dried at room temperature: a colloidal solution was placed into a Petri dish and was kept in a pressure tight vessel containing moisture adsorbents. After drying, the products of the synthesis procedures (1) and (3) produced solid flexible films of composites. Unlike these two, drying of the solution synthesized by the procedure (2) led to the formation of powder-like substance.

Morphology and sizes of NPs were studied by the transmission microscopy method using JEM-100SX electronic microscope at the accelerating voltage 100 keV. The samples for these studies were prepared by drying the droplet of colloidal solution containing NPs on the copper grating. The spatial resolution of the microscopic image was 0.7 nm.

Absorption and photoluminescence (PL) spectra of the solid films of composites were studied using the grating spectrometer MDR-23 and laser with the emission wavelength 375 nm.

3. Results and discussion

It is known that optical absorption studies are widely used to control average size and size distribution of NPs [9, 10]. Since the organic components (PVP and CTAB) are transparent in the visible range, the emerging absorption in this spectral range can be used as an instrument to control the formation of semiconductor phase in the colloid. The spectral position of the absorption features of the colloid relative to the absorption edge of the bulk semiconductor serves for estimation of the NPs average size [11, 12].

Fig. 1 shows the spectral dependence of the optical density $D(\lambda)$ of the colloidal solutions PVP/nanoparticles CdS:Mn and CTAB/nanoparticles CdS:Mn. Both spectra demonstrate a knee in the absorption edge region. It is also seen that the absorption edge of the CTAB/nanoparticles CdS:Mn solution is blue-shifted as compared to the PVP/nanoparticles CdS:Mn solution.

The values of the band gap (E_g) for PVP-coated and CTAB-coated CdS:Mn nanoparticles were calculated using the formula [11]:

$$\Delta E = E_{g(NP)} - E_{g(bulk)} =$$
$$= \frac{\hbar^2 \pi^2}{2R^2} \left[\frac{1}{m_e} + \frac{1}{m_h} \right] - \frac{1.8 e^2}{\varepsilon R} + P . \qquad (1)$$
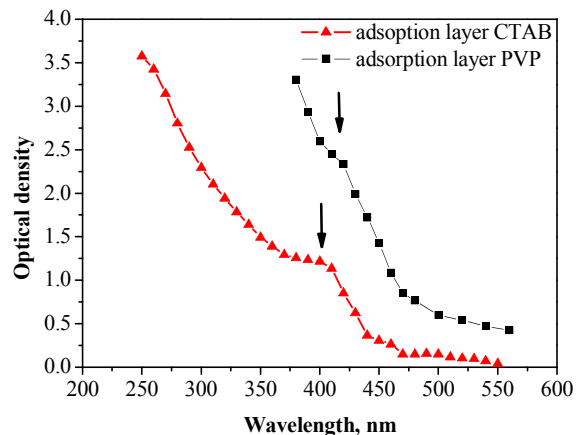

Fig. 1. Spectral dependence of the optical density of colloidal solutions of nanoparticles CdS:Mn synthesized in PVP and CTAB.
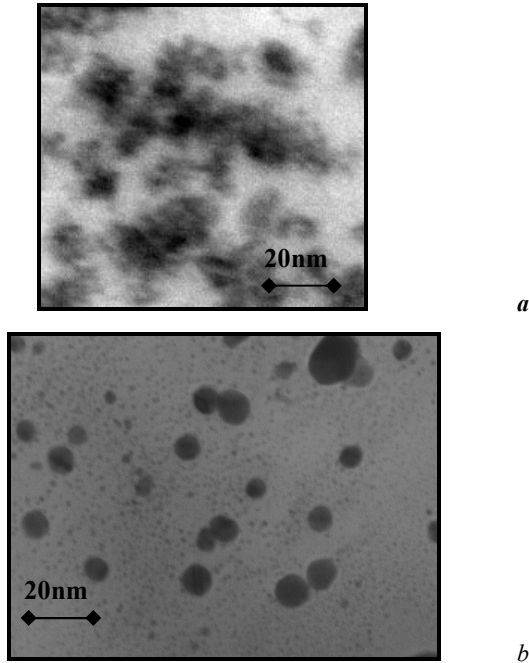
Fig. 2. Electron-microscopic image of CdS:Mn NPs grown in PVP solution (*a*) and CdS:Mn/CTAB NPs grown in CTAB (*b*).

Here, we used $m_e = 0.21$; $m_h = 0.8$; $\varepsilon = 5.4$ for bulk CdS. Note that the influence of the doping with Mn on the band gap value as well as on the electron and hole effective masses is neglected, because, as it is known for bulk CdS:Mn, the low concentration of Mn^{2+} ions <0.5% causes noticeable changes neither in the band gap nor in the effective masses. The values of E_g for PVP-coated and CTAB-coated CdS:Mn nanoparticles obtained from the absorption spectra are 2.7 та 2.8 eV, respectively. The average radius values of the NPs estimated using (1) are equal to 5.8 and 5 nm for PVP-coated and CTAB-coated CdS:Mn NPs, respectively.

We have compared the results of NPs sizes estimation by the optical method with the results of transmitting electron microscopy (TEM) measurements. The latter method provides visualization of NPs and, thus, gives possibility to directly measure the NPs sizes and their dispersion. However, it should be noted that the special preparation of the samples is necessary for TEM measurements, which implies drying of the colloids on the metal gratings (see Section 2). Consequently, depending on the type of adsorbed surface layer, NPs can self-organize into various agglomerates during the drying process. Fig. 2 shows TEM images of CdS:Mn NPs grown in PVP solution (a) and CdS:Mn/CTAB NPs grown in CTAB (b). In these images, NPs are seen as dark spots on the background of light polymeric matrix. It is also seen that NPs grown in PVP tend to agglomerate, while the presence of CTAB surfactant on the surface of NPs helps to avoid agglomeration of NPs during drying the solution on the copper grating.

We have also studied PL of the nanocomposites under the conditions of band-to-band excitation of NPs. Fig. 3 demonstrates PL spectra of NPs grown by synthesis procedures (1) to (3) (see Section 2) and, respectively, have different structures of the adsorptive layers.

A general feature of the PL spectra of all types of NPs, independently on the composition of the growth solution, is the presence of two very wide bands. As will be discussed below, the relative contribution of these two bands strongly depends on the conditions on the surface of NPs (Fig. 3, curves 2 to 4). Large width of PL bands is frequently observed for various colloidal NPs. It is generally accepted that the broadening of PL features in the spectra of NPs results from their size distribution as well as from the influence of organic surrounding, while the origin of the PL bands is still under debates. The high-energy (HE) band in the spectra is usually attributed to the shallow traps [13-16]. In our samples, the radiative transitions within the organic component of nanocomposite can also contribute to PL in the studied spectral region (see the PL spectrum of PVP, curve 1 in Fig. 3). This contribution can be seen either as a weak shoulder on the high-energy wing (spectra 2, 3, and 4) or even as a pronounced peak (spectrum 5), both of them being the emission not related to NPs.

The low-energy (LE) PL band, that is most pronounced in the PL spectrum of CdS:Mn NPs synthesized in CTAB and is seen only as a shoulder in the spectrum of CdS:Mn NPs synthesized *in situ* in PVP, is a compound band, too [13]. At least two types of light-emitting transitions contribute to this band. They are the interatomic transitions of *d*-electrons in Mn ions and localized states on the surface of NPs [13, 17]. The latter states inevitably emerge on any surfaces due to the presence of many disrupted crystal bonds. The contribution of these surface states is more important in NPs as compared to bulk crystals because the surface-to-bulk ratio increases with the decrease of the particle size.
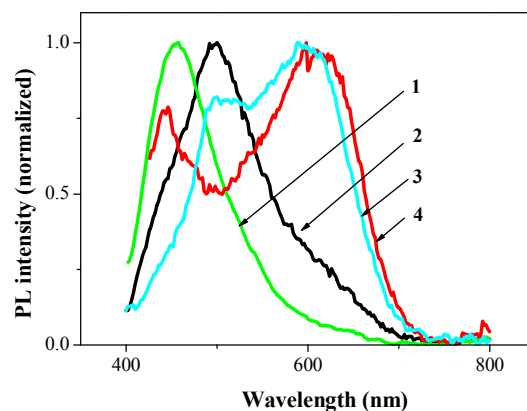

Fig. 3. Photoluminescence spectra: *1* – solution of the PVP polymer; *2* – CdS:Mn NPs synthesized *in situ* in the solution of PVP; *3* – CdS:Mn NPs synthesized in the mixture PVP+CTAB; *4* – CdS:Mn NPs covered with the bilayer of CTAB. All the spectra are normalized to unity at the maximum of intensity.
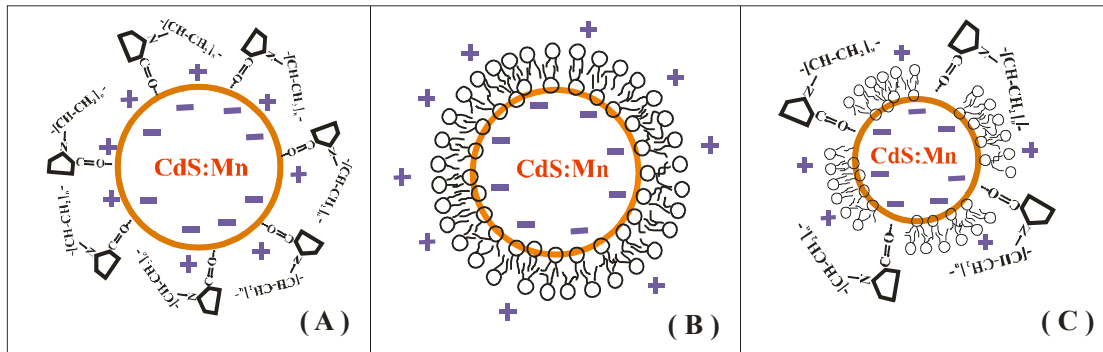
Fig. 4. Structure of the adsorptive layers on the surface of CdS:Mn NPs: a) CdS:Mn/PVA interface (NPs synthesized *in situ* in PVP solution); b) CdS:Mn/double layer CTA⁺(1)-CTA⁺(2) (NPs synthesized in the solution of CTAB surfactant); c) CdS:Mn/CTAB-PVP (NPs grown in the mixture PVP+CTAB).
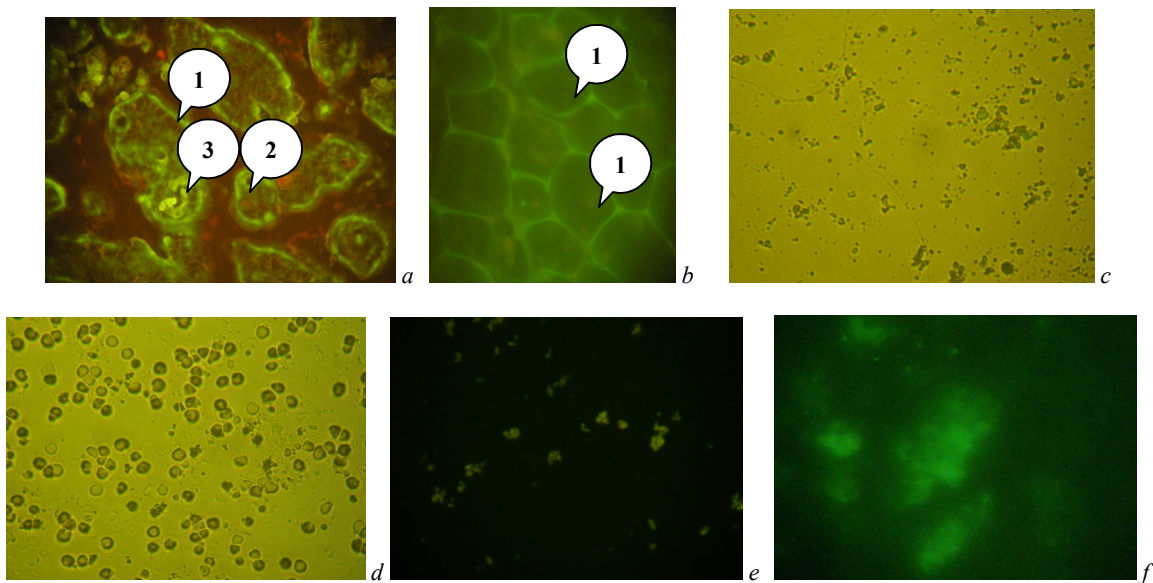

Fig. 5. Images obtained using the optical microscope (*c*) and (*d*) as well as fluorescent microscope (*a*), (*b*), (*e*) and (*f*). (*a*) the fixed tissue of placenta; the distinguished forms are: *1* – trophoblast, *2* – endotheliocyte, *3* – erythrocytes; (*b*) living cells of lipocyte (or adipocyte): *1* – lipocytes, (*c*) washed erythrocytes that were ruined by the injection of CTAB-terminated CdS:Mn NPs; (*d*) and (*e*) – washed erythrocytes that were treated with CdS:Mn NPs terminated with polyvinyl-pyrrolidone; (*f*) visualization of the cells of whole blood treated with CdS:Mn NPs terminated with polyvinyl-pyrrolidone.

Detailed comparison of the spectra of CdS:Mn NPs synthesized *in situ* in PVP, CTAB or in the mixture PVP+CTAB reveals a strong influence of the surface bonding on the light-emitting properties of NPs. To illustrate the changes of the NPs surface conditions, we propose the schemes of the surface bonds shown in Fig. 4. These schemes were drawn taking into account the nature of the functional groups of polymer or surfactant and are used to analyze the influence of the type of adsorptive interaction in the system organic molecule/NP surface on the PL spectra.

The largest difference in the intensity ratio LE/HE is observed between the spectra of NPs grown *in situ* in PVP (Fig. 3, curve 2) and in CTAB (Fig. 3, curve 5). It is seen that the LE band dominates in the spectrum of CTAB-coated NPs. Keeping in mind that the localized states on the surface of NPs [17-19] contribute to the LE band emission, one can suggest that using surfactant for covering the NP surface with the bilayer of CTAB (see Fig. 4b) drastically diminishes the non-radiative quenching of surface-related PL that is characteristic for surface/polymer interface (see Fig. 4a).

The difference between the ratios LE/HE in the spectra of NPs synthesized *in situ* in PVP (Fig. 3, curve 2) and *in situ* in the mixture PVA+CTAB (Fig. 3, curve 3) is less pronounced. The reason for these changes can be the competitive adsorption between the polymer molecules and CTAB ions on the surface of NPs. It is known [20] that under the conditions of competitive adsorption the blocking effect [20] occurs:

the smaller molecules are adsorbed at the initial stages of interaction and hinder further adsorption of bigger molecules. The efficiency of blocking depends on the molecular mass of the polymer: the surfactant almost completely blocks the adsorption of polymers with small molecular mass, does not influence the adsorption of the molecules of average mass and only fragmentary blocks adsorption of the biggest molecules (Fig. 4c) [21]. Thus, under the conditions of competitive adsorption an inhomogeneous surface layer is formed, and non-radiative recombination increases.

We have tested the applicability of the synthesized colloidal solutions of CdS:Mn NPs for biomedical purposes. The type of the surface coverage of NPs is crucial for these studies. We suggested that CdS:Mn NPs with CTAB-terminated surface can be adsorbed on the biomolecules in histological mounts and, thus, can be used for luminescent microscopy studies of certain tissues. Our studies demonstrated that CTAB-terminated CdS:Mn NPs can be efficient for visualization of the structure of placenta and living cells of lipocyte (or adipocyte) (see the images of histological mounts obtained by fluorescent microscope in Figs 5a and 5b, respectively). We have also made the attempts to use these NPs for the studies of native blood. Unfortunately, we observed that these colloidal particles are not applicable for the studies of the native blood because they cause the destruction of the blood cells (see the image of washed erythrocytes in the optical microscope, which demonstrates that they are ruined, Fig. 5c). However, one can avoid the evil action of NPs by varying the NPs surface termination. We have proved that CdS:Mn NPs synthesized in polyvinyl-pyrrolidone are applicable for blood studies. Fig. 5d shows the optical microscope image of washed erythrocytes that were treated with CdS:Mn NPs terminated with polyvinyl-pyrrolidone. It is seen that the erythrocytes remain intact after the injection of latter NPs. Moreover, these NPs preserve their light-emitting properties and can serve for visualization of washed blood cells and even of the cells of the whole blood (see the fluorescent microscope images in Figs 5e and 5f, respectively).

4. Conclusions

We report the synthesis of CdS:Mn NPs in water solutions of polyvinyl-pirrolidone, CTAB surfactant and the mixture polyvinyl-pirrolidone + CTAB. The average radius values obtained by the optical absorption method are 5.8 and 5.0 nm for PVP-coated and CTAB-coated CdS:Mn NPs, respectively. The electron microscopy results support these data and demonstrate the tendency to agglomeration for PVP-coated NPs when drying the solution. The photoluminescence studies of NPs grown in different solutions show that the coverage of the NPs surface with CTAB favors the low-energy emission related to the surface states. The obtained results demonstrate that chemical composition and structure of

the adsorptive layer on the surface of NPs can be used as a technological tool to control light emission of NPs. The possibility to use CdS:Mn NPs grown in PVP as light-emitting labels in biological media has been demonstrated.

References

1. C. de M. Donega, Synthesis and properties of colloidal heteronanocrystals // *Chem. Soc. Rev.* **40**, p. 1512-1546 (2011).
2. A.M. Smith, H. Duan, A.M. Mohs, S. Nie, Bioconjugated quantum dots for in vivo molecular and cellular imaging // *Adv. Drug Delivery Rev.* **60**, p. 1226-1240 (2008).
3. M.J. Brunchez, M. Moronne, P. Gin, S. Weiss, A.P. Alivisatos, Semiconductor nanocrystals as fluorescent biological labels // *Science*, **281**, p. 2013-2016 (1998).
4. W.C.W. Chan and S. Nie, Quantum dot bioconjugates for ultrasensitive nonisotopic detection // *Science*, **281**, p. 2016-2018 (1998).
5. A. Fu, W. Gu, C. Larabell, A.P. Alivisatos // *Current Opinion in Neurobiology*, **15**, p. 568 (2005).
6. J. Kossut, J.A. Gaj (eds.), *Introduction to the Physics of Diluted Magnetic Semiconductors.* Springer Series in Materials Science, **144** (2010).
7. J.K. Oh, Surface modification of colloidal CdX-based quantum dots for biomedical applications // *J. Mater. Chem.* **20**, p. 8433-8445 (2010).
8. A.I. Savchuk, A.G. Voloshchuk, V.I. Fediv, Peculiarities of synthesis of colloidal semimagnetic semiconductor nanoparticles $Cd_{1-x}Mn_xS$ // *Physics and Chemistry of the Solid State*, **10**(1), p. 144-149 (2009).
9. A.P. Alivisatos, Semiconductor clusters, nanocrystals, and quantum dots // *Science*, **271**, p. 933-937 (1996).
10. M. Hosokawa, K. Nogi, M. Naito, T. Yokoyama, *Nanoparticle Technology Handbook.* Elsevier Linacre House, Jordan Hill, Oxford, UK, 2007.
11. Q. Pang, B.C. Guo, C.L. Yang, S.H. Yang, M.L. Gong, W.K. Ge, J.N. Wang, $Cd_{1-x}Mn_xS$ quantum dots: New synthesis and characterization // *J. Cryst. Growth*, **269**, p. 213-217 (2004).
12. S.V. Gaponenko, *Optical Properties of Semiconductor Nanocrystals.* Cambridge University Press, 1998.
13. V.I. Fediv, G.Yu. Rudko, A.I. Savchuk, E.G. Gule, A.G. Voloshchuk, Synthesis route and optical characterization of CdS:Mn/polyvinyl alcohol nanocomposite // *Semiconductor Physics, Quantum Electronics and Optoelectronics*, **15**(2), p. 117-123 (2012).
14. B.A. Harruff, C.E. Bunker, Spectral properties of AOT-protected CdS nanoparticles: Quantum yield enhancement by photolysis // *Langmuir*, **19**, p. 893-897 (2003).

15. C. Huang, C. Wu, S. Li, J. Lai, Y. Zhao, Quantitative model for the surface-related electron transfer in CdS quantum dots // *Chem. Res. Chinese Univ.* **25**(1), p. 17-24 (2009).

16. F. Antolini, E. Trave, L. Mirenghi, M. Re, G. Mattei, L. Tapfer, P. Mazzoldi, CdS and ZnS nanoparticles growth in different reaction media: Synthesis and characterization // *Mater. Res. Soc. Symp. Proc.* **879E**, p. Z3.32.1-Z3.32.7 (2005).

17. X. Ji, H. Li, S. Cheng, Z. Wu, Y. Xie, X. Dong, P. Yan, Growth and photoluminescence of CdS and CdS:Mn nanoribbons // *Mater. Lett.* **65**, p. 2776-2778 (2011).

18. S.V. Rempel, A.A. Razvodov, M.C. Nebogatikov, E.B. Shishkina, V.Ya. Shur, A.A. Rempel, Sizes and fluorescence of cadmium sulfide quantum dots // *Physics of the Solid State,* **55**(3), p. 567-571 (2013).

19. X.S. Zhao, J. Schroeder, P.D. Persans, T.G. Bilodeau, Resonant-Raman-scattering and photoluminescence studies in glass-composite and colloidal CdS // *Phys. Rev. B*, **43**(15), p. 12 580-12 589 (1991).

20. S. Akbar, G. Sarvar, Study of hydrodynamic and non-hydrodynamic interaction parameters for water/PVP/PVA ternary system by solution viscometry // *J. Chem. Soc. Pak.* **32**(3), p. 270-276 (2010).

21. A. Baran, *Polymer-dispersed Systems*. Naukova dumka, Kiev, 1986 (in Russian).